# Deletion of major shell proteins of ethanolamine utilization microcompartment reduces intrinsic antibiotic resistance, biofilm and intracellular survival of *Salmonella* Typhimurium

**Minal R. Bhalerao[1,2†], Aishwarya S. Davkhar[1,2†], Ajit R. Sawant[3], Anindya S. Ghosh[3], Tiffany N. Harris[4], Thomas A. Bobik[4], Ankita Saha[1], Syed G. Dastager[1,2], Sachin A. Agawane[1,2] and Chiranjit Chowdhury[1,2,4*]**

[1]Biochemical Sciences Division, CSIR- National Chemical Laboratory, Pune- 411008, India

[2]Academy of Scientific and Innovative Research (AcSIR), Ghaziabad- 201002, India

[3]Department of Bioscience and Biotechnology, Indian Institute of Technology Kharagpur, Kharagpur-721302, India

[4]Roy J. Carver Department of Biochemistry, Biophysics and Molecular Biology, Iowa State University, Ames, IA, 50011, USA

[†]Contributed Equally to this work

*To whom correspondence should be addressed: Chiranjit Chowdhury, Biochemical Sciences Division, CSIR-National Chemical Laboratory, Dr. Homi Bhabha Road, Pune, MH 411008, India Tel: 020-25902228; Fax- 20-25902648; Email: cchowdhury82@gmail.com

ABSTRACT: With the high rise in *Salmonella* infection and emergence of antibiotic resistant variants, it is imperative to develop novel strategy to control pathogen. Earlier study revealed that *Salmonella* deploys ethanolamine (EA) metabolic machinery to disseminate in the intestine. *Salmonella* with defective in EA metabolism is manifested with lower intestinal colonization efficiency. Remarkably, potential of EA metabolism as therapeutic target is yet to explore. Our study revealed that supplementation of EA and vitamin $B_{12}$ in both rich and minimal media enhanced biofilm formation, increased motility and increased tolerance of *Salmonella* to some antibiotics. Conversely, mutants deficient in EA metabolic enzymes did not exhibit any physiological fitness. In *Salmonella*, EA metabolic enzymes are localized within a proteinaceous microcompartment (MCP) shell composed of thousands copies of shell proteins encoded by five genes from *eut* operon. Intriguingly, bacterial cells with defective MCP shell due to mutation in individual shell protein showed enhanced susceptibility towards a number of antibiotics in minimal media. The shell protein mutants were unable to form biofilms, produced lower curli expression and were defective in flagellar motility. The shell protein mutant also exhibited lower intramacrophagic viability. Notably, phenotypes were restored upon ectopic expression of corresponding genes. It was evident that mutation in the MCP shell protein downregulated the expression of genes related pathogenicity. Overall, this study sheds new light on understanding the relationship between EA metabolism and bacterial physiology that would pave the way of developing novel therapeutic interventions against *Salmonella*.

Cases of gastroenteritis caused by non-typhoidal *Salmonella* (NTS) infection and subsequent deaths are on rise (1, 2) due to acquisition of multiple antibiotic resistance, which has made NTS refractory to commonly used antibiotics (2-10). This opportunistic pathogen has extraordinary capacity to establish colonization and has ability to form biofilms (11-18),

which are advantageous for ensuring its survival in a large range of ecological niches, rendering antibiotic treatment often unsuccessful. Hence, new strategy of infection control is imperative.

Bacterial nutrient metabolisms have long been proposed to serve as therapeutic targets (19, 20). Recent study suggested that the metabolism selectively responsible for *in vivo* growth and dissemination of the pathogen can represent new antimicrobial target (2, 19, 21). It is indicated that ethanolamine (EA) metabolism bestows *Salmonella* with selective proliferation advantage in both aerobic and anaerobic environments (22-25) over natural gut bacteria that mostly do not host this function (26-29).

EA is a break-down product of phosphatidylethanolamine, a phospholipid found in the intestinal epithelium (27). Shedding of enterocytes from the intestinal epithelial cells and the host diets provide rich sources of ethanolamine in the gut environment (27). It is evident that EA metabolism is essential for *Salmonella* fitness in the inflamed intestine and a mutant defective in EA metabolism was documented with less CFU of the pathogen in the spleen, liver and intestine of mice (23). EA utilization also contributes *Salmonella* to disseminate from the intestines to host tissue and drive further systemic infection within it (16, 30). Hence, disruption of EA metabolism could offer a novel infection control measure to combat *Salmonella* infection without dismaying commensals as advocated by several literature (31-33). Remarkably, potential of EA metabolism for future therapeutic development is far less investigated.

Previously, few gene expression studies with other bacteria claimed a link between EA metabolism with cellular motility and biofilm formation (15, 34-37). It is suggested that biofilm formation reflects the potential adhering capability to intestinal surfaces (15, 38) and contributes significantly to pathogenicity and antibiotic resistance (13, 39). EA metabolism may prove to be *Salmonella*'s Achilles' heel; however, direct evidence of EA metabolism on bacterial physiology remains elusive.

In *Salmonella*, the pathway of EA degradation begins with its conversion to ammonia and acetaldehyde by coenzyme-$B_{12}$- dependent ethanolamine ammonia lyase (EAL) encoded by *eutB* and *C* genes (23, 26). Ammonia is utilized as fixed nitrogen for purine and amino acid biosynthesis (40); whereas, acetaldehyde undergoes further processing by acetaldehyde dehydrogenase (EutE) to convert it to acetyl-CoA (26)(Fig. 1). Acetyl-CoA joins the central metabolism such as TCA cycle (energy generation), glyoxylate bypass (carbohydrate synthesis), and lipid biosynthesis. Alternatively, acetaldehyde may be converted to ethanol by alcohol dehydrogenase to maintain cofactor-pool up and running (26, 27) (Fig. 1).

It has been revealed that *Salmonella* encapsulates enzymatic pathways related to EA metabolism within a protein shell, known as ethanolamine utilization microcompartment (Eut MCP) (Fig. 1) (24, 26, 27, 41-44). Eut MCP creates optimum environment for ethanolamine metabolism and provides the bacteria a unique advantage to survive in a hostile environment in the gut (45). The shell of Eut MCP comprises five shell proteins, namely EutS, M, N, L, K (42, 46) that tessellate into facets, edges and vertices of the MCP shell (42, 47, 48) (Fig. 1). Genetic studies reveals the importance of shell proteins in proper MCP assembly (49-52), in retaining metabolic intermediate while selectively control metabolic flux (53) and in the recruitment of enzyme cargo (44, 52, 54). Earlier, deletion of entire MCP shell has been demonstrated to completely abolish EA metabolism in *Salmonella* (49), a phenotype similar to *eutBC* and *eutE* mutants that inactivate key metabolic enzymes (44, 51, 55); indicating pivotal role of MCP shell in the EA metabolism. Recently, individual deletion mutants of *eutM*, *N*, *L* or *eutK* shell protein of *Salmonella* were shown to impair MCP assembly that resulted aberrant MCP morphology and bacterial growth defect (52). It is suggested that EA metabolic function was greatly affected in the shell protein mutants (52).

It has been proposed that disruption of EA metabolism by targeting microcompartment shell assembly could serve as template for future therapeutic design (32). Herein, with the help of molecular genetic technique we constructed individual shell protein mutants in *Salmonella enterica* Typhimurium LT2. The impact of mutations on bacterial physiology, intrinsic antibiotic resistance and intramacrophagic survival are demonstrated.

We envisaged that this study will help in devising better therapeutic strategies to mitigate *Salmonella* infections in future.

## RESULTS

**Deletion of shell proteins makes *Salmonella* susceptible to structurally unrelated antibiotics**

Although minimum inhibitory concentrations (MICs) of some antibiotics had been lower in some shell protein mutants (Table S1); however, changes in the susceptibilities to various antibiotics attributed to shell protein deletion mutation could not be explained by changes in the MICs. Earlier, it has been suggested that the effect of mutation on bacterial growth in presence of antibiotic in respect to wild-type could be better analyzed by determining a relative antibiotic susceptibility index (ASI) (56, 57). To assess intrinsic growth differences between wild-type (WT) *Salmonella enterica* serovar Typhimurium LT2 and its shell protein mutants, a comparative ASI was calculated as the ratio of (mutant $OD_{600}$/WT $OD_{600}$) with antibiotics/(mutant $OD_{600}$/WT $OD_{600}$) without antibiotics, as suggested previously (56, 57). Here, WT *Salmonella* and its shell protein mutants were tested with a variety of antibiotics viz ampicillin, cephalothin, ciprofloxacin, kanamycin, chloramphenicol, cefotaxime and piperacillin. The susceptibility index less than 1 indicates an increased susceptibility against particular antibiotic (Fig. 2). Notably, effect of antibiotics on the growth of shell protein mutants was evident in the No-carbon E minimal media supplemented with vit $B_{12}$ and EA (NE media), not in the rich media like Mueller Hinton (MH) media. It has been observed that loss of shell proteins significantly increased susceptibility of individual mutants to some of the antibiotics (Fig. 2, Fig. S1, S2). Out of all individual shell protein mutants, an *eutL* mutant became sensitive to maximum number of antibiotics tested (Fig. 2, Fig. S1). In contrast, an *eutS* mutant behaved null as compared to other shell protein mutants. Interestingly, ciprofloxacin exhibited maximum activity towards shell protein mutants. It was presumed that EA metabolism might have impeded due to deletion of the individual shell protein (52). To substantiate the relationship between EA metabolism and intrinsic antibiotic resistance, the same test was conducted with *eutB* and *eutKM* mutant against ciprofloxacin. WT *Salmonella* presented more tolerance to ciprofloxacin in presence of media containing EA and $B_{12}$ than that contained glycerol alone. Whereas, an *eutB* mutant with loss of EA metabolism failed to show any fitness even in the presence of EA and $B_{12}$ (Fig. S3), confirming role of EA metabolism in conferring intrinsic antibiotic resistance. Intriguingly, an *eutKM* mutant, where both EutK and EutM shell proteins were deleted also behaved similarly to the *eutB* mutant (Fig. S3). The *eutKM* mutant did not grow in NE media (Fig. S4), presumably due to complete disintegration of Eut MCP assembly that inhibited the

bacteria to utilize ethanolamine. These studies suggested that disruption of Eut MCP shell reduced intrinsic antibiotic resistance of *Salmonella* Typhimurium.

**EA metabolism is impaired in the shell protein mutants**

Microcompartment shell is known to retain the metabolic intermediates and channelizes them to the downstream enzymes in order to keep the metabolic process up and running. Any impairment in the retention of intermediate results in the defects in the metabolism and slower the growth rate. Earlier deletion of individual shell protein breaks Eut MCP assembly and impairs growth in the minimal media supplemented with EA and $B_{12}$ (52). In our study we observed that the most shell protein mutants had poor retention of metabolic intermediate within Eut MCP that gave rise to release of more aldehyde in the media, except *eutK* and *eutS* mutants (Fig. S5). Intriguingly, an *eutL* mutant released highest acetaldehyde among all shell mutant, indicating disruption of the EA metabolism in this mutant compared to wild-type shell protein mutants (Fig. S5), indicating impaired ethanolamine metabolism in the mutants.

**Shell protein mutants have reduced the biofilm forming ability of *Salmonella***

To determine whether reduction of intrinsic antibiotic resistance to various antibiotics was likely to be a function of the impact of individual shell protein mutations on biofilm formation itself, the biofilm forming ability was assessed.

The biofilm was assessed quantitatively by crystal violet staining assay and by live/dead staining followed by their visualization under confocal laser scanning microscopic analyses. Supplementation of EA and vit $B_{12}$ in both Tryptic Soy Broth (TSB) and No-carbon E-glycerol (NG) media enhanced biofilm of wild type *Salmonella* as observed by crystal violet staining assay (Fig. S6). Notwithstanding the visual evidence, the phenotype was subtle in rich media and were quantitatively indistinguishable (Fig. S6a). Conversely, the phenotype was apparent when minimal media was used. It was observed that biofilm of wild-type *Salmonella* was enhanced by ~20% when EA and vit $B_{12}$ were supplemented in NG media (named as NGE media) (Fig S6b, c). Conversely, the addition of the same did not impart much effect in the enzyme mutant where EA metabolism was completely abolished (Fig. S6b, c), indicating relationship between EA utilization and biofilm formation. Interestingly,

an *eutKM* mutant did not show any impact even on addition of EA and vit $B_{12}$ as well (Fig. S6b, c).

Next, we set out to investigate the effect of individual shell protein mutant in biofilm formation. It was observed that phenotype was more discernible in the minimal media with EA serving as carbon source (NE media). All but an *eutS* mutant exhibited reduced biofilm, where maximum reduction (around 73%) was observed in case of an *eutN* mutant (Fig. 3). An *eutL* mutant reduced biofilm by 60%, whereas in case of an *eutM* mutant it was reduced by around 70% as compared to wild-type (Fig. 3). An *eutK* mutant had produced 51% lower biofilm than that of WT (Fig. 3).

To rule out any polar effect, biofilm was set up with the complemented constructs, which demonstrated similar phenotype to that of wild-type (Fig. S7a, b), thereby confirming that mutants were indeed responsible for decreased biofilm.

**Reduced EA metabolic capacity in the shell protein mutants lower curli expression in *Salmonella***

Curli expression has great impact on biofilm formation. Curli fimbriae along with exopolysaccharide (EPS) are known to play crucial roles in cell adhesion and biofilm formation (13, 58-60). Here, we set out to perform congo red agar plate assay in both rich and minimal media. *Salmonella* produces RDAR (red, dry, and rough) morphotype due to production of extracellular polysaccharides (EPS) and curli fimbriae (58). Addition of EA and vit $B_{12}$ in both TYE and glycerol media produced dark red color colony than in TYE and glycerol media alone (Fig. 4a, b). In contrast, mutations in the key metabolic enzymes produced light colored colony (Fig. 4a, b), suggesting strong relationship between EA utilization and curli expression and EPS production. Remarkably, a *eutKM* mutant generating broken shell also produced light colony (Fig. 4a, b). To investigate effect of mutations of individual shell proteins, the assay was performed in NE media, where EA served as a carbon source. It was evident that *eutL*, *eutM* and *eutK* mutants produced light colonies (Fig. 4c) as compared to wild-type. Out of the three, the *eutL* mutant exhibited severe phenotype (Fig. 4). Intriguingly, an *eutN* mutant did not grow well in NE media; however, generated dark red morphotype (Fig. 4). The phenotypes of all individual shell protein mutants were reversed upon complementation with plasmids carrying the respective genes. (Fig. S8)

## An *eutL* mutant produces lower EPS in the minimal media

WT *Salmonella* fluoresced more in UV when EA and $B_{12}$ was supplemented in both rich and minimal media (Fig. 4a, b). Like congo red assay result, the *eutE eutB* and *eutKM* mutants also exhibited lower fluorescence intensity, indicating the role of MCP mediated EA metabolism in EPS production (Fig. 4). To ascertain the effect of individual shell protein mutants on EPS production, the mutants were subjected to grow in NE minimal media supplemented with calcofluor and the fluorescence associated to bacterial suspension was detected after 72 h and quantified using a spectrofluorometer. The synthesis of EPS was greatly affected in *eutL* mutant. This mutant produced around 30% lower EPS than the WT (Fig. 4d). An *eutM* mutant, on the other hand, had produced 9% lower EPS than WT (Fig. 4d). Intriguingly, an *eutN* mutant produced comparatively higher EPS (40% higher) than WT. Knockout of other shell proteins did not show any effect on EPS production (Fig. 4d).

## Swarming motility reduces in the Eut shell protein mutants

The motility is a determining factor in exerting pathogenicity and virulence of bacteria (61). Earlier studies revealed that the strains with lacking flagellar motility exhibit poor biofilm forming ability (62, 63). We set out to demonstrate if deletion of individual shell protein affects swarming motility. Amongst all the shell protein mutants, *eutN*, *eutK* and *eutM* had severely impaired motility (Fig. 5). These mutants had reduced motility by 3 fold as compared to WT. Both *eutL* and *eutS*, on the other hand, produced 2 fold lower swarming motility as compared to WT (Fig. 5a, b). To corroborate the role of EA metabolism on swarming motility, the same has been performed with *eutE*, *eutB* and *eutKM* mutants. Addition of EA and $B_{12}$ enhanced motility of WT *Salmonella* in NGE media. In contrast, presence of EA and $B_{12}$ had no effect in *eutE*, *eutB* and *eutKM* mutants, where EA metabolism was completely lost (Fig. 5c, d), affirming the role of EA metabolism in *Salmonella* motility. The loss of swarming motility in the mutants were reversed upon complementing with the respective genes from the plasmid (Fig. S9).

## Genes involved in biofilm, motility and invasion are downregulated in the shell protein mutants

To evaluate if lower biofilm formation in the shell protein mutants was due to the change in the expression of *luxS* and *csgD*, the expression profile of the same was determined through qRT PCR analyses. It was revealed that the maximum down regulations in the *luxS* and *csgD* gene expression were observed in the sessile cells of the *eutL* and *eutM* mutants. The *luxS* was downregulated by the 92% and 63%, respectively in *eutL* and *eutM*; whereas in case of *csgD*, fold reduction in the respective mutants were 69% and 95% (Fig. 6). By contrast, the *luxS* expression in planktonic cells of *eutL* was reduced by 93% and that in case of *eutM*, it was 86%. While, *csgD* expressions in the planktonic *eutL* and *eutM* cells were downregulated by 95% and 83%, respectively (Fig. 6).

We also set out to determine the expression of motility and invasion related genes. It was indicated that the expression of *fliC*, *fljB* and *motB* was more than 80% downregulated in all the shell protein mutants (Fig. 6). In contrast, maximum downregulation (83%) of *sipA* expression was observed in case of an *eutL* mutant.

To establish the relationship of EA metabolism with the expression of genes related to biofilm, motility and invasion, we sought to determine the expression of *csgD*, *fljB*, *sipA* in minimal media. It was observed that the WT *Salmonella* grown in a minimal media containing EA and $B_{12}$ had slightly higher expression of all the aforementioned genes as compared to the same grown in media without EA as carbon source (Fig. S10). Notably, there were no significant changes in the expression of the above genes in the *eutB*, *eutE* and *eutKM* mutants devoid of enzyme and MCP shell (Fig. S10)

**An *eutL* mutant is less viable than WT in the intramacrophagic environment**

Since, expression study indicated maximum downregulation of *sipA* gene in an *eutL* mutant, we sought to examine the intramacrophagic survival potential of the *eutL* mutant. As ethanolamine utilization operon is known to get inhibited by glucose (64), a modified no-glucose DMEM was used supplemented with 1 mM pyruvate during infection. In the current study invasion defective *Salmonella* (22, 23) were used by constructing an *invA* mutation in the background of WT and mutant strains. To visualize bacteria inside macrophage RAW264.7, the wild-type *Salmonella* and mutants were transformed with a plasmid (pLac22-mCherry). A red fluorescent protein m-Cherry expressing m-Cherry was expressed after the addition of IPTG (1 mM). The bacteria within macrophage were visualized under fluorescent microscope. To determine the counts of phagocytosed bacteria, the macrophages

were washed and subjected to lysis with 0.1 % Triton- X 100. Serial dilutions were plated to determine the viable bacteria as colony forming unit (cfu) $ml^{-1}$ of the cell lysates. Here, viable cfu at the indicated time points were determined as the percentage of this intracellular time 0 h population and normalized such that wild-type was equal to 100%, as depicted earlier (22). It has been observed that the number of recovered bacteria was reduced to 50% in case of *eutL* mutant (Fig. 7a, b). An *eutE* mutant, defective in producing acetaldehyde dehydrogenase had only 40% viable cells remaining (Fig. 7a, b)

## DISCUSSION

Despite several advances in chemotherapy non-typhoidal *Salmonella* (NTS) has become one of the major threats to global public health due to prevalence of multi-drug resistant (MDR) variants. In a list of global priority pathogens for antimicrobial research published by the World Health Organization (WHO), fluoroquinolone and third generation cephalosporine resistant variants have mostly raised a cause of concern (https://www.who.int/news/item/27-02-2017-who-publishes-list-of-bacteria-for-which-new-antibiotics-are-urgently-needed). Additionally, intracellular *Salmonella* Typhimurium are resilient to aminoglycoside antibiotics (65). Eut microcompartment metabolism is proposed to serve as template for designing novel drug to combat against MDR pathogen, as suggested by earlier literature (31, 32). It is suggested that Eut MCP metabolism is an important genomic determinant of pathogenicity associated with gastroenteritis (29) and factor affecting Eut MCP metabolism might interfere with bacterial pathogenesis (32). Albeit several progress in understanding EA metabolism in *Salmonella* (26, 27, 42, 46, 49, 51), the lack of understanding the significance of EA metabolism in bacterial physiology limits the progress to develop novel therapeutics affecting microcompartment metabolism.

The apparent role of EA metabolism modulating bacterial physiology, viability and intrinsic antibiotic resistance could not be established in the nutrient rich media; the condition where most of the modern therapeutics are developed (66). Intriguingly, the phenotype was greatly manifested under minimal media conditions, which created a paradigm shift underscoring the role of Eut MCP metabolism in modulating bacterial physiology. Minimal media supplemented with EA not only provides a validated approximation of the gut environment in which *Salmonella* disseminates during inflammation but also exemplify roles of specific nutrients in the bacterial physiology. The use of minimal media to explore novel antimicrobial targets was also depicted elsewhere (19, 21, 56, 66). Since, mutation of

individual shell protein exhibited small phenotype in the conventional MIC determination; therefore, we conducted growth analysis to capture minor fitness effects of mutations of all the individual shell protein in presence of structurally unrelated antibiotics (56, 57, 67). The antibiotic susceptibility index of the mutants relative to wild-type (ASI) indicates that the deletion of *eutL* and *eutM* imparted great impact on intrinsic antibiotic resistance of *Salmonella*, where maximum sensitivity was observed in an *eutL* mutant (Fig. 2). The EutL and EutM are structurally orthologous to PduB and PduA shell proteins of 1, 2-propanediol utilization microcompartment (Pdu MCP) (26, 48). The former conforms pseudohexameric trimer, whereas the latter forms canonical hexamer (26, 48). Eut MCPs of *Salmonella* had not been purified yet. However, previous literature suggested that hexameric and trimeric shell proteins share maximum percentage of total shell protein content (68); where trimer alone contributes around 50% amongst all shell proteins (68). The trimeric EutL was crystalized in both open and close confirmation and was proposed to allow transport of large molecule through its central pore (48, 53). EutL also interacts with ethanolamine substrate (53). Alternatively, hexameric EutM shell protein is presumed to transport EA substrate (69). Recent study revealed that individual deletion of either EutM or EutL shell protein results growth defect and formation of polar aggregates (52). We presumed that EA metabolism might have been disrupted in *eutL* and *eutM* mutants due to aberrant MCP shell assembly. The release of acetaldehyde intermediate (Fig. S5) resulting severe carbon loss in the single shell protein mutant supports our hypothesis.

It is tempting to observe that genetic mutation on the *eutL* and *eutM* result the bacterial cell susceptible to ciprofloxacin, kanamycin, cefotaxime and chloramphenicol (Fig. 2). It is also revealed that biofilm formation, curli expression and EPS production are reduced in the cell where either of the major MCP shell proteins are lost (Fig. 3). We surmise that EA metabolism upregulates pathogenicity related genes present in *Salmonella* pathogenicity island-1 (SPI-1) that enhances physiological fitness (Fig. S6). Recently, genetic disruption of MCP formation represses fusobacterial pathogenesis and virulence (70). It can be presumed that the heightened biofilm and EPS reduce the permeability of antibiotics. However, reason of null effect of other antibiotics needs to be explored. Notably, inactivation of EA metabolism in *eutL* mutant also render *Salmonella* susceptible to host's innate defense system (Fig. 7). Role of MCP mediated EA utilization in the intracellular survival and replication of *Listeria monocytogenes* has been demonstrated recently (71).

Genetic mutation targeting major shell proteins disrupting EA metabolism would provide great resources in designing future antimicrobials against *Salmonella*. In order to further validate the potential of MCP assembly and metabolism as drug target, we set out to examine the effect of the deletion of a major shell protein, EutL on growth of a chloramphenicol resistant *Salmonella*. In this study, a *cam* cassette was inserted at *invA* chromosomal locus (*invA*::*frt-cam-frt*) of both WT and *eutL* mutant. The bacteria were grown in minimal media supplemented with EA and $B_{12}$ and the growth was monitored in the microplate reader, as mentioned in the methodology section. It has been observed that the $OD_{600}$ of the cell containing secondary mutation at *eutL* declines at comparatively faster rate at increasing chloramphenicol concentration than the cell having EutL shell protein intact (Fig. S11). The current study also provides deep insights on understanding the differential roles of shell proteins in Eut MCP assembly and metabolism.

## MATERIALS AND METHODS

### Chemicals and reagents.

Ethanolamine hydrochloride, vitamin $B_{12}$ (CN-$B_{12}$), glycerol, 3-methyl-2-benzothiazolinone hydrazone hydrochloride (MBTH) and the Congo-red were from Sigma-Aldrich (St. Louis, MO). Antibiotics, crystal violet, Isopropyl-β-D-1-thiogalactopyranoside (IPTG) and arabinose were from Himedia (Mumbai, India). LIVE/DEAD BacLight Bacterial Viability Kit was from Invitrogen (Waltham, MA). Q5 DNA polymerase, restriction enzymes and T4 ligase were New England Biolabs (Beverly, MA). NovaTaq PCR Master Mix was from Merck (Darmstadt, Germany). Other chemicals were obtained from Qualigens Thermofisher Scientific (Powai, India).

### Bacterial strains, media and growth conditions

The bacterial strains used are listed in Table S1. All strains are derived from *Salmonella enterica* serovar Typhimurium strain LT2. The rich medium used was Luria-Bertani/Lennox (lysogeny broth) (LB) medium (Himedia, Mumbai, India). For selecting transformants TYE media was used, where bacto-tryptone, yeast extract and agar were purchased from Himedia Laboratories (Himedia, Mumbai, India). For MIC experiments, overnight cultures were inoculated in cation-adjusted Mueller–Hinton broth (MHB) and subcultured into MHB or the indicated minimal media. For biofilm experiments the rich media used was Tryptic Soy Broth (TSB, Himedia, Mumbai, India) (72). The minimal media used were either no carbon-E (NCE) or no carbon-no nitrogen (NCN) medium (73). Ethanolamine (30 mM) was used as a carbon source in NCE medium, as a nitrogen source in NCN medium with glycerol (20 mM), or as a carbon and nitrogen source in NCN medium (73). Minimal media were supplemented with 1 mM MgSO4, 0.3% each of valine, isoleucine, leucine and threonine and 50 μM ferric citrate (50, 74). CN-$B_{12}$ (150 nM) was employed as exogenous vitamin $B_{12}$ source. Antibiotics were used at the following concentrations: ampicillin, 100 μg/ml and chloramphenicol, 20 μg/ml. Solid media were prepared by adding agar (1.5%, Himedia) to LB, TYE, NCE, or NCN medium.

### Construction of deletion mutants and complemented Strains

All primers and plasmids used in this study are listed in Table S2. Chromosomal deletion of individual Eut MCP shell proteins was constructed by recombineering as followed earlier (50, 75, 76). In brief, chloramphenicol cassette flanking FRT sequence was amplified from pKD3 plasmid in such a way that the amplicon contains portions of sequences adjacent to the gene to be deleted. The amplicon was electroporated into the cell expressing λ-Red recombinase from plasmid pKD46. Transformants were screened against chloramphenicol (20 µg/mL) on TYE-Cam agar plates. The antibiotic cassette was crossed off by expressing flippase from a plasmid pCP20. In order to make double mutants, the chloramphenicol cassette at respective gene loci was moved to another mutant by transduction as previously described (74, 75), using phage P22 HT105 int. For complementation studies, the genes encoding Eut shell proteins were cloned in pLac22 plasmid within *Bgl*II and *Hin*dIII sites as stated earlier (50). All the clones and mutants were confirmed by PCR followed by sequencing.

**Antibiotic susceptibility assays of various classes of antibiotics**

Initially, the antibiotic sensitivity experiment was carried out in the agar diffusion assay (both MHB and minimal media supplemented with 30 mM EA and 150 nM $B_{12}$) using EZY-MIC strips (Himedia) of structurally unrelated classes of antibiotics, such as ampicillin, cefalotin, chloramphenicol, ciprofloxacin, cefotaxime, kanamycin and piperacillin. Minimum inhibitory concentration (MIC) based on Epsilometer method (E-test) was used to determine the antimicrobial sensitivity of the WT *Salmonella* and individual shell protein mutants. Later, broth dilution method was adopted to enhance the sensitivity of the test. The concentration range of antibiotics for the broth dilution method was obtained from the agar diffusion assay. The micro-broth dilution assay was performed in 96- well micro-titer plates according to the Clinical and Laboratory Standards Institute (CLSI) guidelines (77). Overnight cultures were inoculated from a single colony into LB and subcultured 1:100 into the cation adjusted MHB supplemented with 30 mM EA and 150 nM $B_{12}$ and grown to log phase ($OD_{600}$1.0). Cultures were next diluted into either cation adjusted MHB or in the aforementioned minimal media for a starting inoculum of ~$1 \times 10^5$ CFU/ml. The antibiotics were two-fold serially diluted and the total volume was made up to 200 µl. Assay plates were incubated for 24 h at 37 $^{o}$C with double orbital shaking. The growth was monitored with a BioTek Epoch 2 Microplate Spectrophotometer (Agilent). The assay was replicated four times and atleast three biological replicates. The MIC was calculated based on the concentration that inhibited bacterial growth

>90% compared to the no antibiotic control. To determine for intrinsic growth differences between WT and individual shell protein mutants, a relative antimicrobial susceptibility index (ASI) was calculated, which can be calculated as the ratio of (mutant $OD_{600}$/wild-type $OD_{600}$) in presence of antibiotics/ (mutant $OD_{600}$/wild-type $OD_{600}$) without antibiotics. ASI values less than 1 indicate an increased antimicrobial susceptibility.

**Determination of Biofilm formation by crystal violet assay**

Biofilm formation assay was performed as described earlier with some modifications (78). Overnight cultures of wild-type *Salmonella*, its mutants and the cells harboring their respective plasmid clones were diluted into 1:100 in TSB and were allowed to grow until $OD_{600}$ reached to 0.5. The cells were preinduced for microcompartment formation with ethanolamine (30 mM) and $B_{12}$ (150 nM). The culture was further diluted into biofilm growth media (either TSB or minimal media supplemented with ethanolamine and $B_{12}$) into 96-well polystyrene plates to an $OD_{600}$ 0.1 and incubated at 37 °C for 72 h under static conditions. The genes from the respective plasmid clones were expressed by inducing with 20 uM IPTG. After incubating the plates for 72 h, the wells were washed twice with phosphate-buffered saline (PBS), and the biofilms were fixed at 80 °C for 15 min followed by staining with 0.5 % crystal violet (CV) for 15 min. The excess stain was rinsed with distilled water and then air dried. The bound CV on the biofilms was solubilized by 33% acetic acid (v/v) and measured at $OD_{570}$ using Epoch microplate spectrophotometer (Agilent-BioTek, USA). The biofilm formation index was calculated as BFI= (AB-CW)/(GB-GW), where AB is $OD_{570}$ of the stained test well; CW is $OD_{570}$ of the stained control well; GB is $OD_{600}$ of the planktonic cells; GW is $OD_{600}$ of the control well (79).

**Microscopic analysis of biofilm structures**

The CV-stained biofilm in the microplate was observed under 40X objective of Labomed TCM400 microscope. Bacterial viability within the biofilm structures was determined by staining the biofilm samples in coverslip with LIVE/DEAD BacLight Bacterial Viability Kit (Invitrogen, MA) as per manufacturer's instruction. After washing the biofilm with PBS, the stained samples were viewed under a confocal laser scanning microscope (Leica Stellaris, Germany) at 20× magnification. The images were captured and processed with the help of

LASx software to determine the thickness of the biofilm matrix and the bacterial viability within its structure.

The biofilm architecture was also determined with the help of field-emission scanning electron microscopy (FE-SEM). Samples were prepared by washing the air-dried biofilm containing cover slips with PBS followed by fixation with 2.5 % glutaraldehyde. Samples were gold-coated and finally subjected to visualization under a FEI Nova Nano 450 field emission scanning electron microscope and images were captured at 5000 × magnification.

**Assessment of *Salmonella* morphotypes by congo red agar plate assay**

The curli morphotypes of wild-type *Salmonella* and its mutants were screened in Congo red agar (CRA) plate as stated earlier (80) with some modifications. Overnight bacterial cultures in LB were diluted to secondary culture media (LB supplemented with 30 mM ethanolamine and 150 nM cyanocobalamin) at a ratio of 1:100. Next, optical density (OD) of the cultures were adjusted to an $OD_{600}$ ~ 0.2 with phosphate buffered saline and next spot inoculated (5 µl) onto Tryptone-Yeast extract (No NaCl) agar plate or in the minimal media agar plate supplemented with EA and $B_{12}$, as stated before. Congo red (40 mg/L) (Sigma-Aldrich, St. Louis, MO, USA) was added in the media as mentioned earlier (80). The colony morphology and the color were monitored after 96 h of incubation at 37 °C.

**Calcofluor assay for EPS production**

Bacterial EPS production was assessed in calcofluor agar plate as discussed earlier with some modifications (80). Overnight cultures of WT *Salmonella* and respective mutants were diluted to 1:100 in LB supplemented with 30 mM ethanolamine and 150 nM cyanocobalamin and were grown for 6 h at 37 °C. The optical density of all the cultures was adjusted to ~ 0.1 before streaking onto the calcofluor-agar plates supplemented with 1 mg/ml calcofluor white (HiMedia). Plates were incubated at 37 °C for 72 h, and fluorescence intensity was monitored under a UV light source. EPS production was also quantified by measuring the calcofluor bound to cells as described previously (80). Fluorescence measurements were performed in a Fluorescence Spectrophotometer (Promega) with excitation at 360 nm and the emission at 460 nm. The fluorescent intensity in arbitrary unit was normalized with the $OD_{600}$ of the bacterial suspension and represented with respect to that of WT. Data are mean values of triplicate determinations plotted with standard error with mean.

## Motility Assay

For swarming motility behavior studies, the concentration of agar used in the media was 0.6% (w/v). Different combinations of minimal medium were used where ethanolamine served as source of carbon or nitrogen or both. Overnight cultures of WT *Salmonella* and respective mutants were diluted to 1:100 in LB supplemented with 30 mM ethanolamine and 150 nM cyanocobalamin ($B_{12}$) and were grown for 6 h at 37 °C. One microliter of the culture with OD600 ~ 0.1 was spotted onto the minimal medium agar plates. After 72 h incubation period, the swarming pattern was observed and the diameter was measured.

## RNA extraction and qPCR analysis

Total RNA was extracted both from biofilm-dwelling bacterial cells and the cells from the swarming agar plates. Both planktonic and sessile cells from biofilm plates and cells from swarming plates were resuspended in 500 µL PBS. Double volume of RNAprotect bacterial reagent (Qiagen, Hilden, Germany) was added to stabilize RNA prior to isolation. RNA was extracted using the RNeasy Mini Kit (Qiagen, Hilden, Germany) according to manufacturer's instruction. RNA purity was determined by measuring the $A_{260}/A_{280}$ absorbance ratio and the concentration was determined with SimpliNano Spectrophotometer (GE Health Care, UK). RNA was converted to cDNA using Ecodry Premix (Random Hexamers, Takara, Japan). The cDNA was amplified using the Applied Biosystems 2x SybrGreen Master Mix as per manufacturer's protocol by consensus primers detecting the expression genes related to biofilm, motility as stated in Table S2. Primers were designed using Primer 3, GeneRunner and Multiple Primer Analyzer (Thermo Fisher Scientific) to ensure no cross-reactivity to other genes in the *Salmonella* LT2 chromosome. Amplicon length was approximately 150-200bp. Reactions were run using the StepOnePlus RT-qPCR machine (Applied Biosystems, USA). Three technical replicates were averaged for analysis by the relative quantification method in which $C_T$ values were normalized to the reference genes *rpoA* and *gyrA*. The expression level of the target genes was compared using the relative quantification method. Data were presented as the change (n-fold) in expression levels compared to WT levels. Error bars represent the standard deviations of the $2^{-\Delta\Delta CT}$ value.

## Estimation of acetaldehyde

For acetaldehyde measurement, the wild type and *eut* shell protein mutants were grown in 1 ml of minimal medium containing 30 mM ethanolamine and 150 nM of cyanocobalamin. The culture was incubated in 5 ml sterile glass vials containing rubber caps were sealed with aluminum caps with the help of crimper tool. The glass vials were incubated at 37°C for 12 h. 286 µl of 100 mM Potassium Citrate buffer (pH 3.6), 143 µl of 0.1% MBTH (3-Methyl-2-Benzothiazolinone Hydrazone) and 246 µl of double deionized water were pre-added to a 48 well plate (VWR). 40 µl of the sample was collected from each vial using a sterile syringe without opening the cap of the glass vial and added to the respective well. The plate was incubated at 37°C for 15 mins at static condition. After incubation, the sample in the wells were diluted by addition of 285 µl of double deionized water. The absorbance of the samples was measured at 305 nm in the microplate reader as described previously (81).

## Bacterial infection in macrophages

The RAW264.7 murine macrophage cell lines were grown and maintained in Dulbecco's Modified Eagle Medium (DMEM) with 10 % Fetal Bovine Serum and penicillin-streptomycin solution at 37 °C in 5 % carbon dioxide. The macrophage cells were grown in modified DMEM media supplemented with FBS (10%), ethanolamine (30 mM), vitamin $B_{12}$ (150 nm), and Sodium pyruvate (1 mM) for the infection experiment. Overnight cultures of both wild-type and mutants of *Salmonella* in LB broth were diluted 1:100 in LB media supplemented with ethanolamine and vitamin $B_{12}$ and allowed to grow until the mid-log phase. The bacterial cells were harvested and diluted to $OD_{600}$ 0.1. RAW264.7 macrophages were infected with these bacteria at a multiplicity of infection 50:1 and centrifuged at 1000 rpm for 5 min to aid the adhesion of bacterial cells to the macrophage and the plates were kept undisturbed for 60 min at 37 °C in 5 % carbon dioxide.

## Microscopic analysis of bacterial viability within infected macrophages

To visualize bacterial cells inside the macrophage RAW264.7 the wild-type and mutants were transformed with a plasmid (pLac22-mCherry) expressing mCherry (Red fluorescence) after the addition of IPTG (1 mM). The infection of the macrophage was done as explained in the above section. Briefly, one hour after infection to the RAW264.7 cells with *Salmonella* strains the media was replaced by gentamycin (100 µg/ml) containing DMEM

media to kill the non-internalized bacterial cells and incubated for 1 h. Further, the media containing gentamicin were replaced with DMEM media without any antibiotic and incubated for 2 h. The macrophage cells were washed gently with PBS to remove any non-internalized bacteria before being subjected to imaging. The fluorescence microscopic images of the viable bacteria within macrophages were captured using a fluorescence microscope with the Excitation/Emission for mCherry: 587/610 nm.

## SUPPLEMENTAL MATERIAL

Supplemental material is available online only

## ACKNOWLEDGMENTS

This study was mostly supported by the ad-hoc research grant from Indian Council of Medical Research (ICMR) [Diarr/Adhoc/5/2022-ECD-II] to C.C., S.G.D. and A.S.G. Authors also thank SERB-Ramanujan fellowship grant (SB/S2/RJN-128/2017) for initial support. M.R.B. and A.S.D. acknowledge Council of Scientific and Industrial Research (CSIR) and Department of Biotechnology, Govt. of India (DBT), respectively for their fellowships. Authors thank Ms. Yashodhara Shinde for her tireless help in constructing secondary mutation at *invA* gene in WT, *eutL* and *eutE* mutant cells. Authors thank National Collection of Industrial Microorganisms (NCIM), CSIR-National Chemical Laboratory, Pune, India for nucleotide sequencing and other services.

## Author contributions

**MRB**: Performed bacterial genetics, physiology and molecular biology work, carried out microscopic visualization and data analyses, wrote original draft; **ASD**: Performed molecular biology work, gene expression analysis, confocal microscopic analyses; **ARS**: Cell culture work and fluorescence microscopy; **ASG**: Investigation, formal analysis of cell culture work and funding acquisition; **TNH**: Performed molecular biology work; **TAB**: Supervision, formal analyses and initial resources; **AS**: Biofilm work; **SGD**: Supervision and funding acquisition; **SBA**: Supervision, **CC**: Conceptualization, initial molecular biology and genetics work, Supervision, Funding acquisition, Project administration, Supply of resources, Writing - review & editing.

## References


1. Ingle DJ, Ambrose RL, Baines SL, Duchene S, Goncalves da Silva A, Lee DYJ, Jones M, Valcanis M, Taiaroa G, Ballard SA, Kirk MD, Howden BP, Pearson JS, Williamson DA. 2021. Evolutionary dynamics of multidrug resistant Salmonella enterica serovar 4,[5],12:i:- in Australia. Nat Commun 12:4786.
2. Sutar AA, Dashpute RS, Shinde YD, Mukherjee S, Chowdhury C. 2024. A Systemic Review on Fitness and Survival of Salmonella in Dynamic Environment and Conceivable Ways of Its Mitigation. Indian J Microbiol 64:267–286.
3. Collaborators GBDN-TSID. 2019. The global burden of non-typhoidal salmonella invasive disease: a systematic analysis for the Global Burden of Disease Study 2017. Lancet Infect Dis 19:1312-1324.
4. Crump JA, Sjolund-Karlsson M, Gordon MA, Parry CM. 2015. Epidemiology, Clinical Presentation, Laboratory Diagnosis, Antimicrobial Resistance, and Antimicrobial Management of Invasive Salmonella Infections. Clin Microbiol Rev 28:901-37.
5. Cuypers WL, Jacobs J, Wong V, Klemm EJ, Deborggraeve S, Van Puyvelde S. 2018. Fluoroquinolone resistance in Salmonella: insights by whole-genome sequencing. Microb Genom 4.
6. D VTN, Venkitanarayanan K, Kollanoor Johny A. 2018. Antibiotic-Resistant Salmonella in the Food Supply and the Potential Role of Antibiotic Alternatives for Control. Foods 7.
7. Dzeyie KA, Dhanapaul S, Rubeshkumar P, Desing S, Vignesh MS, Raveendran I, Kumar P, Kathuria S, Choudhary S, Saroha E, Siromany V, Raju M, Ganeshkumar P, Ponnaiah M, Sodha SV, Laserson K, Bhatnagar T, Kapoor L, Bahl A, Jain SK, Gupta S, Murhekar MV, Singh SK. 2021. Outbreak of ceftriaxone-resistant Salmonella enterica serotype Typhi-Tiruchirappalli, Tamil Nadu, India, June 2018. IJID Reg 1:60-64.
8. Majowicz SE, Musto J, Scallan E, Angulo FJ, Kirk M, O'Brien SJ, Jones TF, Fazil A, Hoekstra RM, International Collaboration on Enteric Disease 'Burden of Illness S. 2010. The global burden of nontyphoidal Salmonella gastroenteritis. Clin Infect Dis 50:882-9.
9. Tacconelli E, Carrara E, Savoldi A, Harbarth S, Mendelson M, Monnet DL, Pulcini C, Kahlmeter G, Kluytmans J, Carmeli Y, Ouellette M, Outterson K, Patel J, Cavaleri M, Cox EM, Houchens CR, Grayson ML, Hansen P, Singh N, Theuretzbacher U, Magrini N, Group WHOPPLW. 2018. Discovery, research, and development of new antibiotics: the WHO priority list of antibiotic-resistant bacteria and tuberculosis. Lancet Infect Dis 18:318-327.
10. Xiang Y, Li F, Dong N, Tian S, Zhang H, Du X, Zhou X, Xu X, Yang H, Xie J, Yang C, Liu H, Qiu S, Song H, Sun Y. 2020. Investigation of a Salmonellosis Outbreak Caused by Multidrug Resistant Salmonella Typhimurium in China. Front Microbiol 11:801.

11. Krause KM, Serio AW, Kane TR, Connolly LE. 2016. Aminoglycosides: An Overview. Cold Spring Harb Perspect Med 6.
12. Menashe O, Kaganskaya E, Baasov T, Yaron S. 2008. Aminoglycosides affect intracellular Salmonella enterica serovars typhimurium and virchow. Antimicrob Agents Chemother 52:920-6.
13. Aleksandrowicz A, Carolak E, Dutkiewicz A, Blachut A, Waszczuk W, Grzymajlo K. 2023. Better together-Salmonella biofilm-associated antibiotic resistance. Gut Microbes 15:2229937.
14. Wang X, Biswas S, Paudyal N, Pan H, Li X, Fang W, Yue M. 2019. Antibiotic Resistance in Salmonella Typhimurium Isolates Recovered From the Food Chain Through National Antimicrobial Resistance Monitoring System Between 1996 and 2016. Front Microbiol 10:985.
15. MacKenzie KD, Palmer MB, Koster WL, White AP. 2017. Examining the Link between Biofilm Formation and the Ability of Pathogenic Salmonella Strains to Colonize Multiple Host Species. Front Vet Sci 4:138.
16. Oshota O, Conway M, Fookes M, Schreiber F, Chaudhuri RR, Yu L, Morgan FJE, Clare S, Choudhary J, Thomson NR, Lio P, Maskell DJ, Mastroeni P, Grant AJ. 2017. Transcriptome and proteome analysis of Salmonella enterica serovar Typhimurium systemic infection of wild type and immune-deficient mice. PLoS One 12:e0181365.
17. Tassinari E, Duffy G, Bawn M, Burgess CM, McCabe EM, Lawlor PG, Gardiner G, Kingsley RA. 2019. Microevolution of antimicrobial resistance and biofilm formation of Salmonella Typhimurium during persistence on pig farms. Sci Rep 9:8832.
18. Trampari E, Holden ER, Wickham GJ, Ravi A, Martins LO, Savva GM, Webber MA. 2021. Exposure of Salmonella biofilms to antibiotic concentrations rapidly selects resistance with collateral tradeoffs. NPJ Biofilms Microbiomes 7:3.
19. Ali MM, Newsom DL, Gonzalez JF, Sabag-Daigle A, Stahl C, Steidley B, Dubena J, Dyszel JL, Smith JN, Dieye Y, Arsenescu R, Boyaka PN, Krakowka S, Romeo T, Behrman EJ, White P, Ahmer BM. 2014. Fructose-asparagine is a primary nutrient during growth of Salmonella in the inflamed intestine. PLoS Pathog 10:e1004209.
20. Stokes JM, Lopatkin AJ, Lobritz MA, Collins JJ. 2019. Bacterial Metabolism and Antibiotic Efficacy. Cell Metab 30:251-259.
21. Johnson JW, Ellis MJ, Piquette ZA, MacNair C, Carfrae L, Bhando T, Ritchie NE, Saliba P, Brown ED, Magolan J. 2022. Antibacterial Activity of Metergoline Analogues: Revisiting the Ergot Alkaloid Scaffold for Antibiotic Discovery. ACS Med Chem Lett 13:284-291.
22. Anderson CJ, Clark DE, Adli M, Kendall MM. 2015. Ethanolamine Signaling Promotes Salmonella Niche Recognition and Adaptation during Infection. PLoS Pathog 11:e1005278.

23. Thiennimitr P, Winter SE, Winter MG, Xavier MN, Tolstikov V, Huseby DL, Sterzenbach T, Tsolis RM, Roth JR, Baumler AJ. 2011. Intestinal inflammation allows Salmonella to use ethanolamine to compete with the microbiota. Proc Natl Acad Sci U S A 108:17480-5.
24. Kaval KG, Garsin DA. 2018. Ethanolamine Utilization in Bacteria. mBio 9.
25. Srikumar S, Fuchs TM. 2011. Ethanolamine utilization contributes to proliferation of Salmonella enterica serovar Typhimurium in food and in nematodes. Appl Environ Microbiol 77:281-90.
26. Chowdhury C, Sinha S, Chun S, Yeates TO, Bobik TA. 2014. Diverse bacterial microcompartment organelles. Microbiol Mol Biol Rev 78:438-68.
27. Garsin DA. 2010. Ethanolamine utilization in bacterial pathogens: roles and regulation. Nat Rev Microbiol 8:290-5.
28. Moore TC, Escalante-Semerena JC. 2016. The EutQ and EutP proteins are novel acetate kinases involved in ethanolamine catabolism: physiological implications for the function of the ethanolamine metabolosome in Salmonella enterica. Mol Microbiol 99:497-511.
29. Tsoy O, Ravcheev D, Mushegian A. 2009. Comparative genomics of ethanolamine utilization. J Bacteriol 191:7157-64.
30. Ormsby MJ, Logan M, Johnson SA, McIntosh A, Fallata G, Papadopoulou R, Papachristou E, Hold GL, Hansen R, Ijaz UZ, Russell RK, Gerasimidis K, Wall DM. 2019. Inflammation associated ethanolamine facilitates infection by Crohn's disease-linked adherent-invasive Escherichia coli. EBioMedicine 43:325-332.
31. Krysenko S, Wohlleben W. 2022. Polyamine and Ethanolamine Metabolism in Bacteria as an Important Component of Nitrogen Assimilation for Survival and Pathogenicity. Med Sci (Basel) 10.
32. Prentice MB. 2021. Bacterial microcompartments and their role in pathogenicity. Curr Opin Microbiol 63:19-28.
33. Zhou J, Xiong X, Wang K, Zou L, Lv D, Yin Y. 2017. Ethanolamine Metabolism in the Mammalian Gastrointestinal Tract: Mechanisms, Patterns, and Importance. Curr Mol Med 17:92-99.
34. Delmas J, Gibold L, Fais T, Batista S, Leremboure M, Sinel C, Vazeille E, Cattoir V, Buisson A, Barnich N, Dalmasso G, Bonnet R. 2019. Metabolic adaptation of adherent-invasive Escherichia coli to exposure to bile salts. Sci Rep 9:2175.
35. Miller AL, Nicastro LK, Bessho S, Grando K, White AP, Zhang Y, Queisser G, Buttaro BA, Tukel C. 2021. Nitrate Is an Environmental Cue in the Gut for Salmonella enterica Serovar Typhimurium Biofilm Dispersal through Curli Repression and Flagellum Activation via Cyclic-di-GMP Signaling. mBio 13:e0288621.

36. Watve S, Barrasso K, Jung SA, Davis KJ, Hawver LA, Khataokar A, Palaganas RG, Neiditch MB, Perez LJ, Ng WL. 2020. Parallel quorum-sensing system in Vibrio cholerae prevents signal interference inside the host. PLoS Pathog 16:e1008313.
37. Zhang S, Morgan X, Dogan B, Martin FP, Strickler S, Oka A, Herzog J, Liu B, Dowd SE, Huttenhower C, Pichaud M, Dogan EI, Satsangi J, Longman R, Yantiss R, Mueller LA, Scherl EJ, Sartor RB, Simpson KW. 2022. Mucosal metabolites fuel the growth and virulence of E. coli linked to Crohn's disease. JCI Insight 7.
38. Siddique A, Azim S, Ali A, Andleeb S, Ahsan A, Imran M, Rahman A. 2021. Antimicrobial Resistance Profiling of Biofilm Forming Non Typhoidal Salmonella enterica Isolates from Poultry and Its Associated Food Products from Pakistan. Antibiotics (Basel) 10.
39. Long J, Yang C, Liu J, Ma C, Jiao M, Hu H, Xiong J, Zhang Y, Wei W, Yang H, He Y, Zhu M, Yu Y, Fu L, Chen H. 2024. Tannic acid inhibits Escherichia coli biofilm formation and underlying molecular mechanisms: Biofilm regulator CsgD. Biomed Pharmacother 175:116716.
40. Khatri N, Khatri I, Subramanian S, Raychaudhuri S. 2012. Ethanolamine utilization in Vibrio alginolyticus. Biol Direct 7:45; discussion 45.
41. Bobik TA, Lehman BP, Yeates TO. 2015. Bacterial microcompartments: widespread prokaryotic organelles for isolation and optimization of metabolic pathways. Mol Microbiol 98:193-207.
42. Pokhrel A, Kang SY, Schmidt-Dannert C. 2021. Ethanolamine bacterial microcompartments: from structure, function studies to bioengineering applications. Curr Opin Microbiol 62:28-37.
43. Cheminay C, Chakravortty D, Hensel M. 2004. Role of neutrophils in murine salmonellosis. Infect Immun 72:468-77.
44. Costa FG, Escalante-Semerena JC. 2022. Localization and interaction studies of the Salmonella enterica ethanolamine ammonia-lyase (EutBC), its reactivase (EutA), and the EutT corrinoid adenosyltransferase. Mol Microbiol 118:191-207.
45. Jakobson CM, Tullman-Ercek D. 2016. Dumpster Diving in the Gut: Bacterial Microcompartments as Part of a Host-Associated Lifestyle. PLoS Pathog 12:e1005558.
46. Kofoid E, Rappleye C, Stojiljkovic I, Roth J. 1999. The 17-gene ethanolamine (eut) operon of Salmonella typhimurium encodes five homologues of carboxysome shell proteins. J Bacteriol 181:5317-29.
47. Kerfeld CA, Aussignargues C, Zarzycki J, Cai F, Sutter M. 2018. Bacterial microcompartments. Nat Rev Microbiol 16:277-290.
48. Tanaka S, Sawaya MR, Yeates TO. 2010. Structure and mechanisms of a protein-based organelle in Escherichia coli. Science 327:81-4.

49. Brinsmade SR, Paldon T, Escalante-Semerena JC. 2005. Minimal functions and physiological conditions required for growth of salmonella enterica on ethanolamine in the absence of the metabolosome. J Bacteriol 187:8039-46.

50. Cheng S, Sinha S, Fan C, Liu Y, Bobik TA. 2011. Genetic analysis of the protein shell of the microcompartments involved in coenzyme B12-dependent 1,2-propanediol degradation by Salmonella. J Bacteriol 193:1385-92.

51. Penrod JT, Roth JR. 2006. Conserving a volatile metabolite: a role for carboxysome-like organelles in Salmonella enterica. J Bacteriol 188:2865-74.

52. Yang M, Adegbite O, Chang P, Zhu X, Li Y, Dykes GF, Chen Y, Savage N, Hinton JCD, Lian L, Liu L. 2024. Molecular basis of the biogenesis of a protein organelle for ethanolamine utilization. bioRxiv doi:10.1101/2024.05.17.594633:2024.05.17.594633.

53. Thompson MC, Cascio D, Leibly DJ, Yeates TO. 2015. An allosteric model for control of pore opening by substrate binding in the EutL microcompartment shell protein. Protein Sci 24:956-75.

54. Choudhary S, Quin MB, Sanders MA, Johnson ET, Schmidt-Dannert C. 2012. Engineered protein nano-compartments for targeted enzyme localization. PLoS One 7:e33342.

55. Stojiljkovic I, Baumler AJ, Heffron F. 1995. Ethanolamine utilization in Salmonella typhimurium: nucleotide sequence, protein expression, and mutational analysis of the cchA cchB eutE eutJ eutG eutH gene cluster. J Bacteriol 177:1357-66.

56. Russo TA, Carlino-MacDonald U, Alvarado CL, Davies CJ, Barnes O, Trivedi G, Mathur P, Hutson A, Adams FG, Zang M, Ascari A, Eijkelkamp BA. 2023. Penicillin Binding Protein 7/8 Is a Potential Drug Target in Carbapenem-Resistant Acinetobacter baumannii. Antimicrob Agents Chemother 67:e0103322.

57. Atwood DN, Beenken KE, Lantz TL, Meeker DG, Lynn WB, Mills WB, Spencer HJ, Smeltzer MS. 2016. Regulatory Mutations Impacting Antibiotic Susceptibility in an Established Staphylococcus aureus Biofilm. Antimicrob Agents Chemother 60:1826-9.

58. Cimdins A, Simm R. 2017. Semiquantitative Analysis of the Red, Dry, and Rough Colony Morphology of Salmonella enterica Serovar Typhimurium and Escherichia coli Using Congo Red. Methods Mol Biol 1657:225-241.

59. Kaiser TD, Pereira EM, Dos Santos KR, Maciel EL, Schuenck RP, Nunes AP. 2013. Modification of the Congo red agar method to detect biofilm production by Staphylococcus epidermidis. Diagn Microbiol Infect Dis 75:235-9.

60. Pawar DM, Rossman ML, Chen J. 2005. Role of curli fimbriae in mediating the cells of enterohaemorrhagic Escherichia coli to attach to abiotic surfaces. J Appl Microbiol 99:418-25.

61. Lou F, Wang K, Hou Y, Shang X, Tang F. 2023. Inhibitory effect of resveratrol on swimming motility and adhesion ability against Salmonella enterica serovar Typhimurium infection. Microb Pathog 184:106323.
62. Vilas Boas D, Castro J, Araujo D, Nobrega FL, Keevil CW, Azevedo NF, Vieira MJ, Almeida C. 2024. The Role of Flagellum and Flagellum-Based Motility on Salmonella Enteritidis and Escherichia coli Biofilm Formation. Microorganisms 12.
63. Wang F, Deng L, Huang F, Wang Z, Lu Q, Xu C. 2020. Flagellar Motility Is Critical for Salmonella enterica Serovar Typhimurium Biofilm Development. Front Microbiol 11:1695.
64. Kaval KG, Gebbie M, Goodson JR, Cruz MR, Winkler WC, Garsin DA. 2019. Ethanolamine Utilization and Bacterial Microcompartment Formation Are Subject to Carbon Catabolite Repression. J Bacteriol 201.
65. Lo JH, Kulp SK, Chen CS, Chiu HC. 2014. Sensitization of intracellular Salmonella enterica serovar Typhimurium to aminoglycosides in vitro and in vivo by a host-targeted antimicrobial agent. Antimicrob Agents Chemother 58:7375-82.
66. Brown ED, Wright GD. 2016. Antibacterial drug discovery in the resistance era. Nature 529:336-43.
67. Yano H, Nakata N, Yahara K, Sugai M, Sato Y. 2025. Specific variants in ftsI reduce carbapenem susceptibility in Pseudomonas aeruginosa. Microbiol Spectr doi:10.1128/spectrum.01027-25:e0102725.
68. Havemann GD, Bobik TA. 2003. Protein content of polyhedral organelles involved in coenzyme B12-dependent degradation of 1,2-propanediol in Salmonella enterica serovar Typhimurium LT2. J Bacteriol 185:5086-95.
69. Slininger Lee MF, Jakobson CM, Tullman-Ercek D. 2017. Evidence for Improved Encapsulated Pathway Behavior in a Bacterial Microcompartment through Shell Protein Engineering. ACS Synth Biol 6:1880-1891.
70. Franklin DS, Chen YW, Chen Y, Wittchen M, Agnew A, Luu A, Whitelegge JP, Zhou ZH, Tauch A, Das A, Ton-That H. 2025. Ethanolamine-induced assembly of microcompartments is required for Fusobacterium nucleatum virulence. mBio 16:e0340524.
71. Chatterjee A, Kaval KG, Garsin DA. 2024. Role of ethanolamine utilization and bacterial microcompartment formation in Listeria monocytogenes intracellular infection. Infect Immun 92:e0016224.
72. Gonzalez JF, Tucker L, Fitch J, Wetzel A, White P, Gunn JS. 2019. Human Bile-Mediated Regulation of Salmonella Curli Fimbriae. J Bacteriol 201.
73. Sheppard DE, Penrod JT, Bobik T, Kofoid E, Roth JR. 2004. Evidence that a B12-adenosyl transferase is encoded within the ethanolamine operon of Salmonella enterica. J Bacteriol 186:7635-44.

74. Chowdhury C, Chun S, Sawaya MR, Yeates TO, Bobik TA. 2016. The function of the PduJ microcompartment shell protein is determined by the genomic position of its encoding gene. Mol Microbiol 101:770-83.

75. Chowdhury C, Bobik TA. 2019. Engineering the PduT shell protein to modify the permeability of the 1,2-propanediol microcompartment of Salmonella. Microbiology (Reading) 165:1355-1364.

76. Datsenko KA, Wanner BL. 2000. One-step inactivation of chromosomal genes in Escherichia coli K-12 using PCR products. Proc Natl Acad Sci U S A 97:6640-5.

77. Institute CaLS. 2024. Methods for Dilution Antimicrobial Susceptibility Tests for Bacteria That Grow Aerobically, 12th Edition ed. CLSI, Wayne, PA.

78. Tursi SA, Puligedda RD, Szabo P, Nicastro LK, Miller AL, Qiu C, Gallucci S, Relkin NR, Buttaro BA, Dessain SK, Tukel C. 2020. Salmonella Typhimurium biofilm disruption by a human antibody that binds a pan-amyloid epitope on curli. Nat Commun 11:1007.

79. Martinez-Medina M, Naves P, Blanco J, Aldeguer X, Blanco JE, Blanco M, Ponte C, Soriano F, Darfeuille-Michaud A, Garcia-Gil LJ. 2009. Biofilm formation as a novel phenotypic feature of adherent-invasive Escherichia coli (AIEC). BMC Microbiol 9:202.

80. Paytubi S, Cansado C, Madrid C, Balsalobre C. 2017. Nutrient Composition Promotes Switching between Pellicle and Bottom Biofilm in Salmonella. Front Microbiol 8:2160.

81. Ochoa JM, Dershwitz P, Schappert M, Sinha S, Herring TI, Yeates TO, Bobik TA. 2023. A single shell protein plays a major role in choline transport across the shell of the choline utilization microcompartment of Escherichia coli 536. Microbiology (Reading) 169.

## Figures

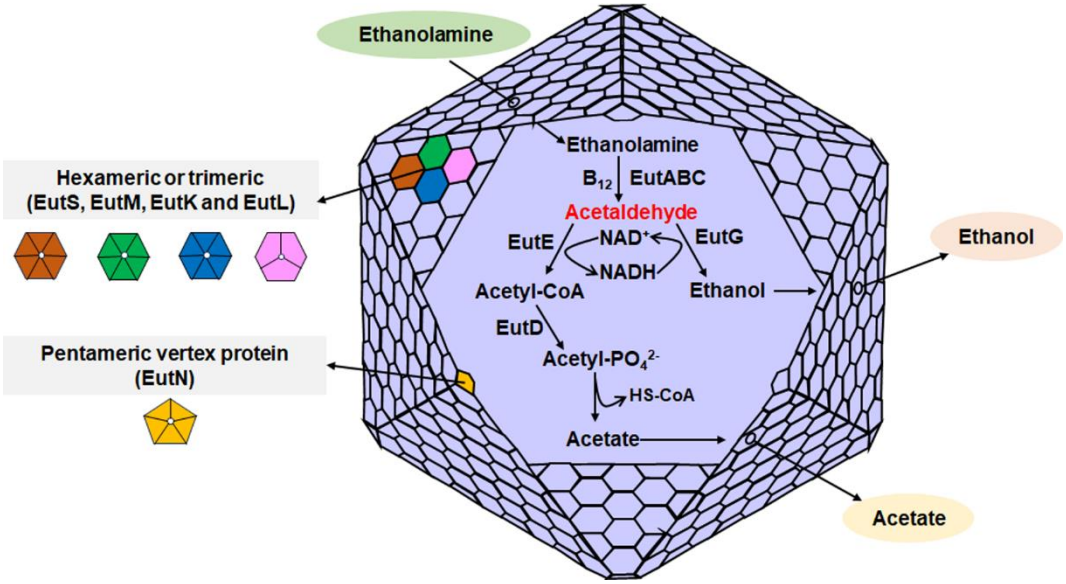


**Fig. 1**. Functional model of Ethanolamine Utilization Microcompartment (Eut MCP).

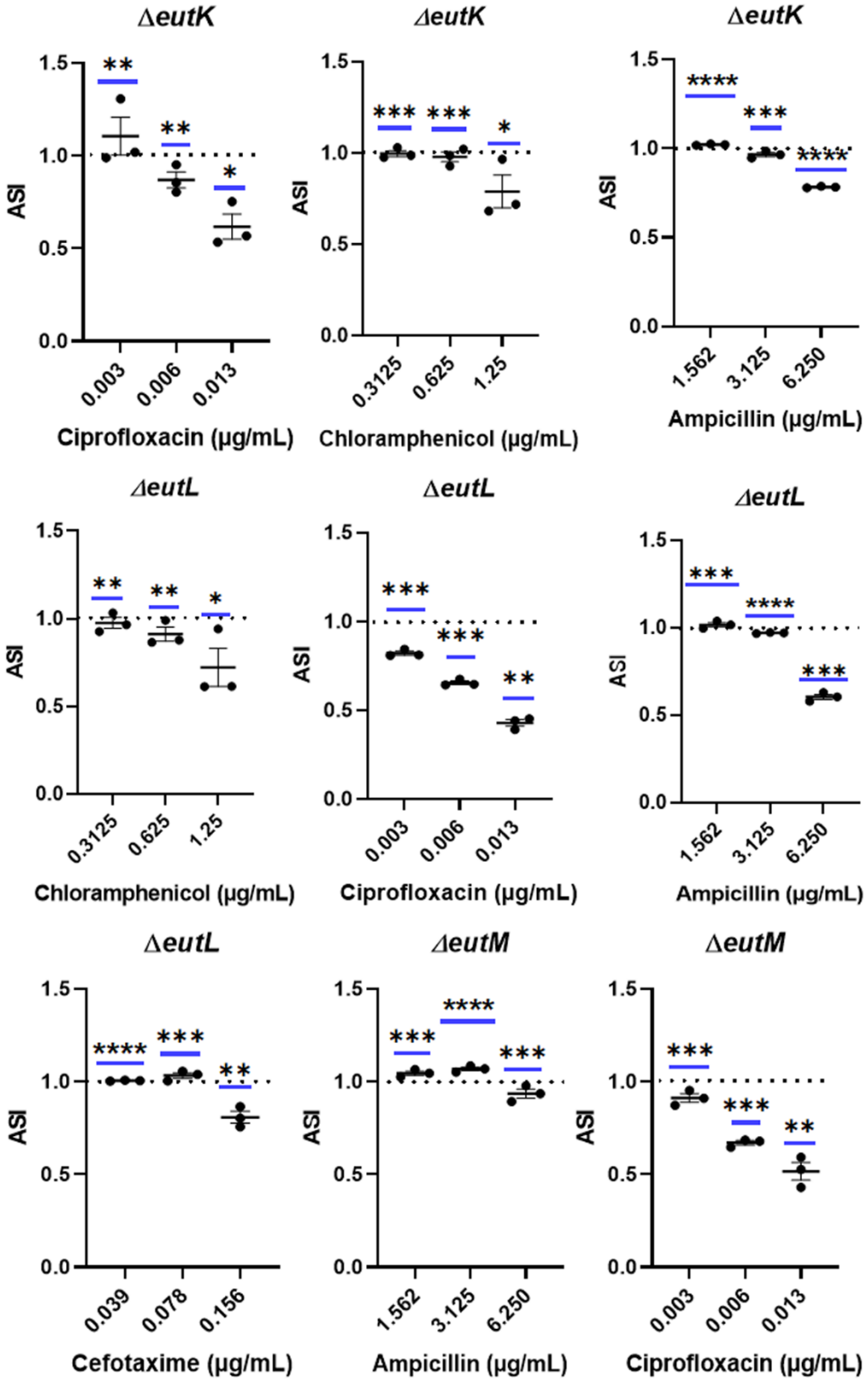
ΔeutK
ΔeutK
ΔeutK
ΔeutL
ΔeutL
ΔeutL
ΔeutL
ΔeutM
ΔeutM
ASI
1.5
1.0
0.5
0.0
0.003
0.006
0.013
Ciprofloxacin (μg/mL)
0.3125
0.625
1.25
Chloramphenicol (μg/mL)
1.562
3.125
6.250
Ampicillin (μg/mL)
0.039
0.078
0.156
Cefotaxime (μg/mL)

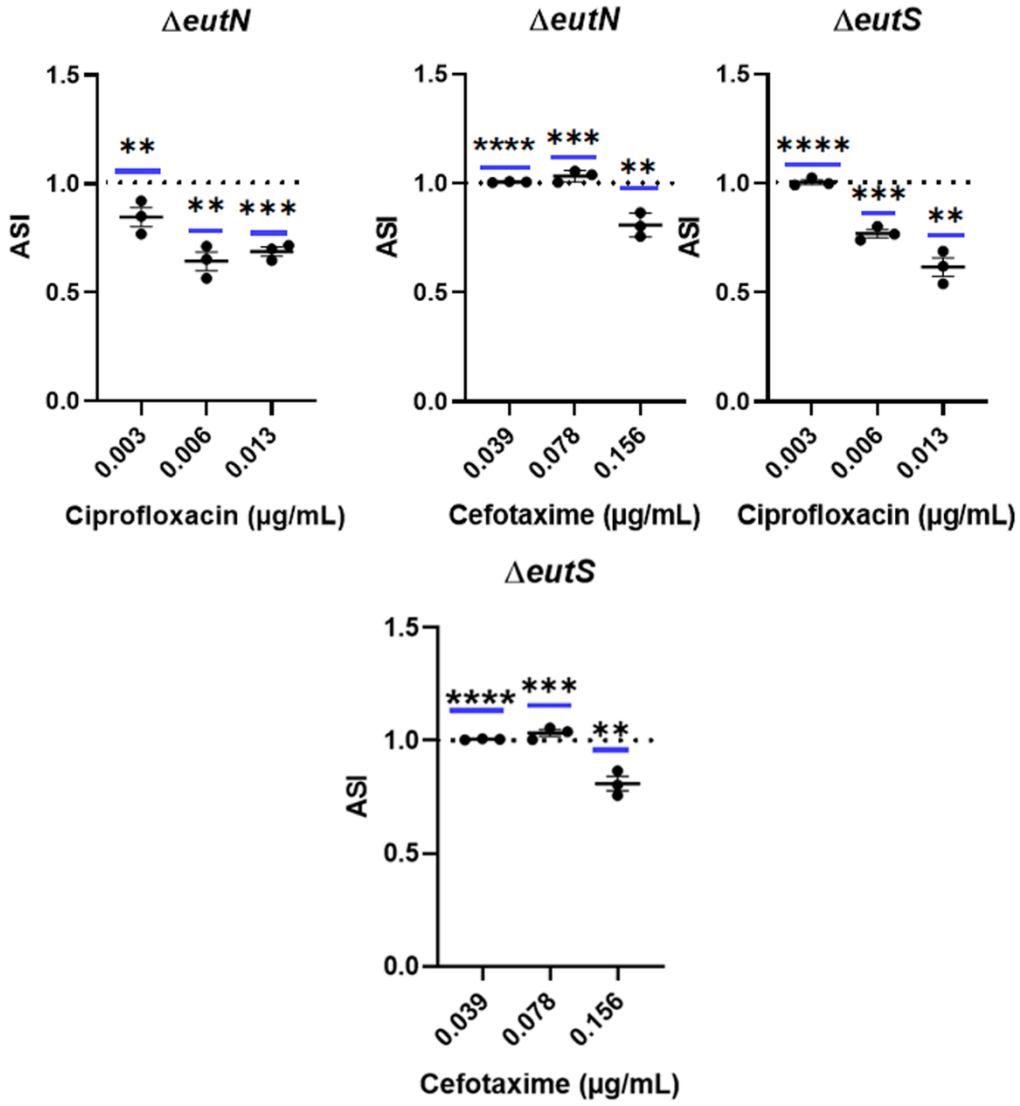


**Fig. 2**. Antibiotic Susceptibility of Wild Type and Shell Protein Mutants of *Salmonella* in the presence of various antibiotics. The various antimicrobials' activity was assessed against WT and Eut shell protein mutants as defined by growth measured by optical density (Å600) after 24 h at 37°C in NCE supplemented with 30mM ethanolamine, 150nM Vit. $B_{12}$, and 0.5mM glycerol. Each symbol represents a biological replicate. Three biological replicates and four technical replicates were performed for each antimicrobial. The antibiotic susceptibility index (ASI) is the ratio of (mutant Å600/wild-type Å600) with antimicrobial/ (mutant Å600/wild-type Å600) without antimicrobial. ASI values of 1 indicate an increased antimicrobial susceptibility for Mutants. NS, $P > 0.05$; *, $P \leq 0.05$; **, $P \leq 0.01$; ***, $P \leq 0.001$; ****, $P \leq 0.0001$ (one-sample t and Wilcoxon tests).

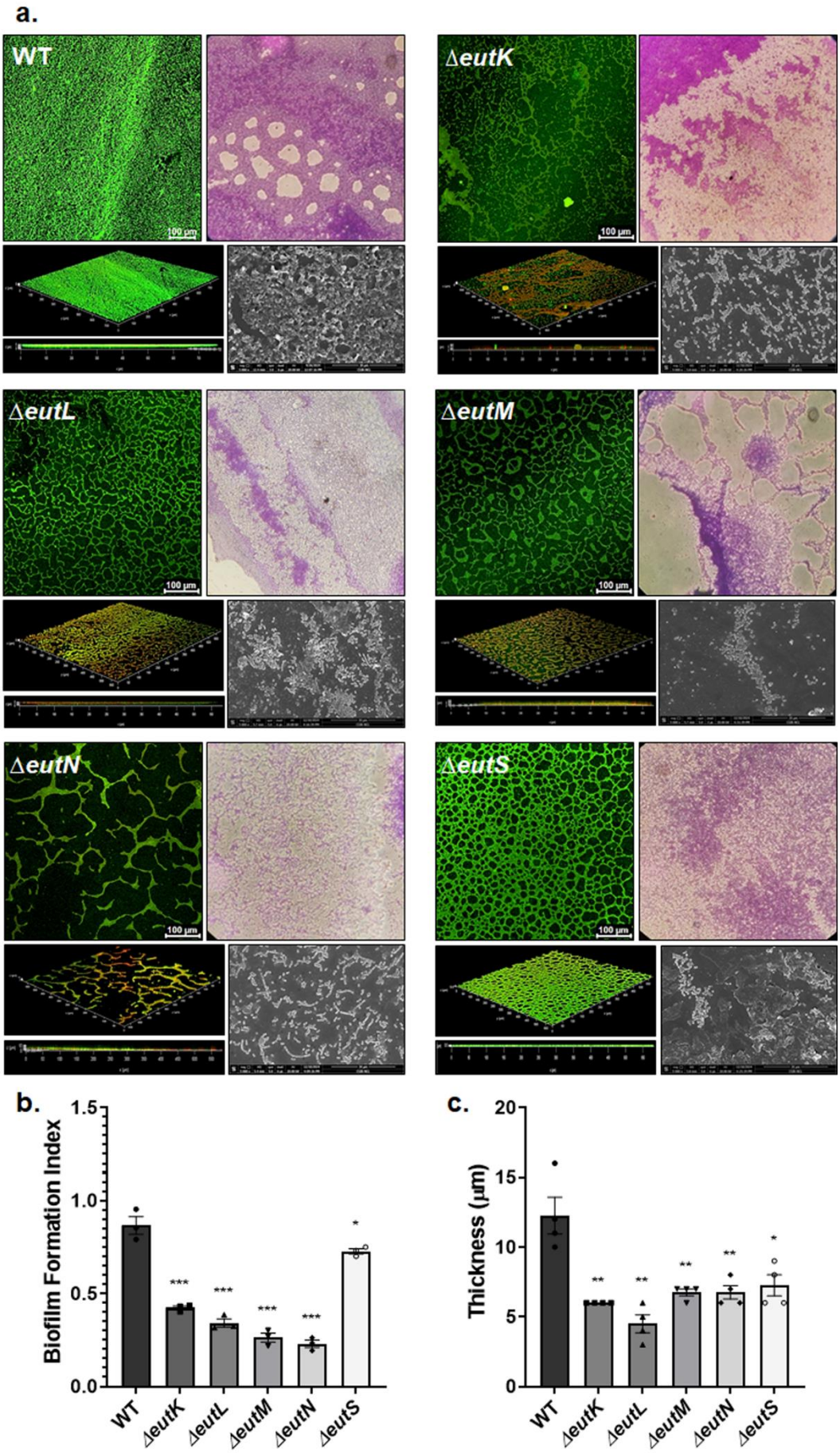
a.
WT
ΔeutK
ΔeutL
ΔeutM
ΔeutN
ΔeutS
100 µm
b.
Biofilm Formation Index
1.5
1.0
0.5
0.0
***
*
WT
ΔeutK
ΔeutL
ΔeutM
ΔeutN
ΔeutS
c.
Thickness (µm)
20
15
10
5
0
**
*

860

**Fig. 3**. a) Evaluation of biofilm through confocal, crystal violet, and FE-SEM analyses. The samples were stained with SYTO9 (green, live) and propidium iodide (red, dead) for confocal microscopy and visualized under a 20X objective. Orthogonal views of both Z-stacks and 3D images are presented. b) The biofilm formation index (BFI) was calculated using the Crystal Violet assay. c) The thickness of the biofilm was measured in 3D images of the confocal. An unpaired t-test (two-tailed) was used for statistical significance. NS $P > 0.05$, * $P < 0.05$, ** $P < 0.01$, *** $P < 0.001$, **** $P < 0.0001$ compared to the wild type control.

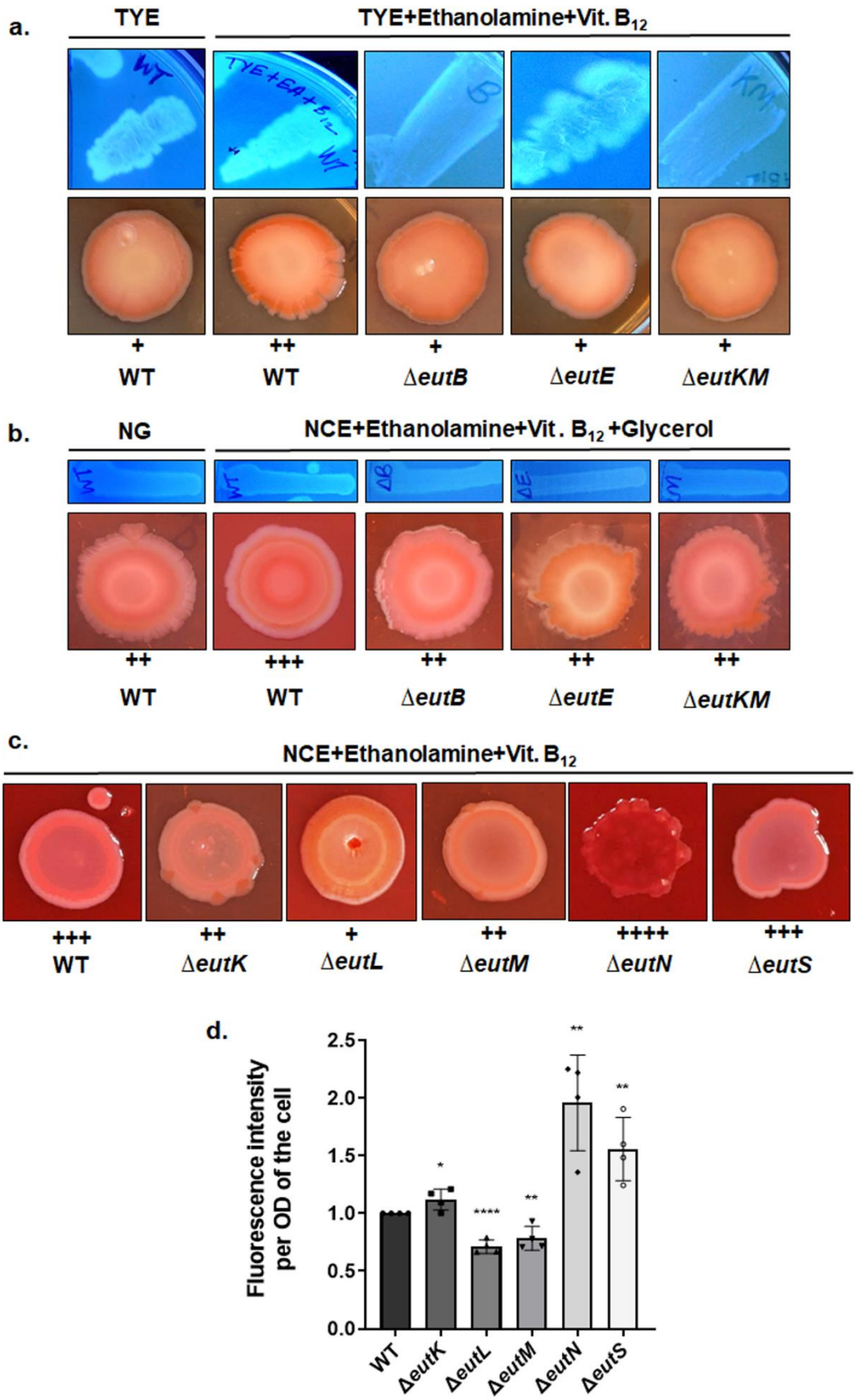
a.
TYE
TYE+Ethanolamine+Vit. B12
+
WT
++
WT
+
ΔeutB
+
ΔeutE
+
ΔeutKM
b.
NG
NCE+Ethanolamine+Vit. B12 +Glycerol
++
WT
+++
WT
++
ΔeutB
++
ΔeutE
++
ΔeutKM
c.
NCE+Ethanolamine+Vit. B12
+++
WT
++
ΔeutK
+
ΔeutL
++
ΔeutM
++++
ΔeutN
+++
ΔeutS
d.
Fluorescence intensity per OD of the cell
2.5
2.0
1.5
1.0
0.5
0.0
WT
ΔeutK
ΔeutL
ΔeutM
ΔeutN
ΔeutS

868

869

**Fig. 4**. Morphotypes of *S. enterica* after 96h incubation at 37°C on Congo Red agar and Calcofluor Agar. a) TYE and TYE Supplemented with 30mM Ethanolamine and 150 nM Vitamin $B_{12}$. b) NCE+Glycerol and NCE+Glycerol supplemented with 30mM Ethanolamine and 150 nM Vitamin $B_{12}$. c) Ethanolamine acts as a carbon source, with the media being NCE, 30mM ethanol, and 150 nM vitamin $B_{12}$. d) Quantify EPS using Calcofluor Fluorescent Assay. An unpaired *t*-test (two-tailed) was used for statistical significance. + = White, ++ = Pink, and +++ = Red Color morphology. * $P < 0.05$, ** $P < 0.01$, *** $P < 0.001$, **** $P < 0.0001$ compared to the wild type control.

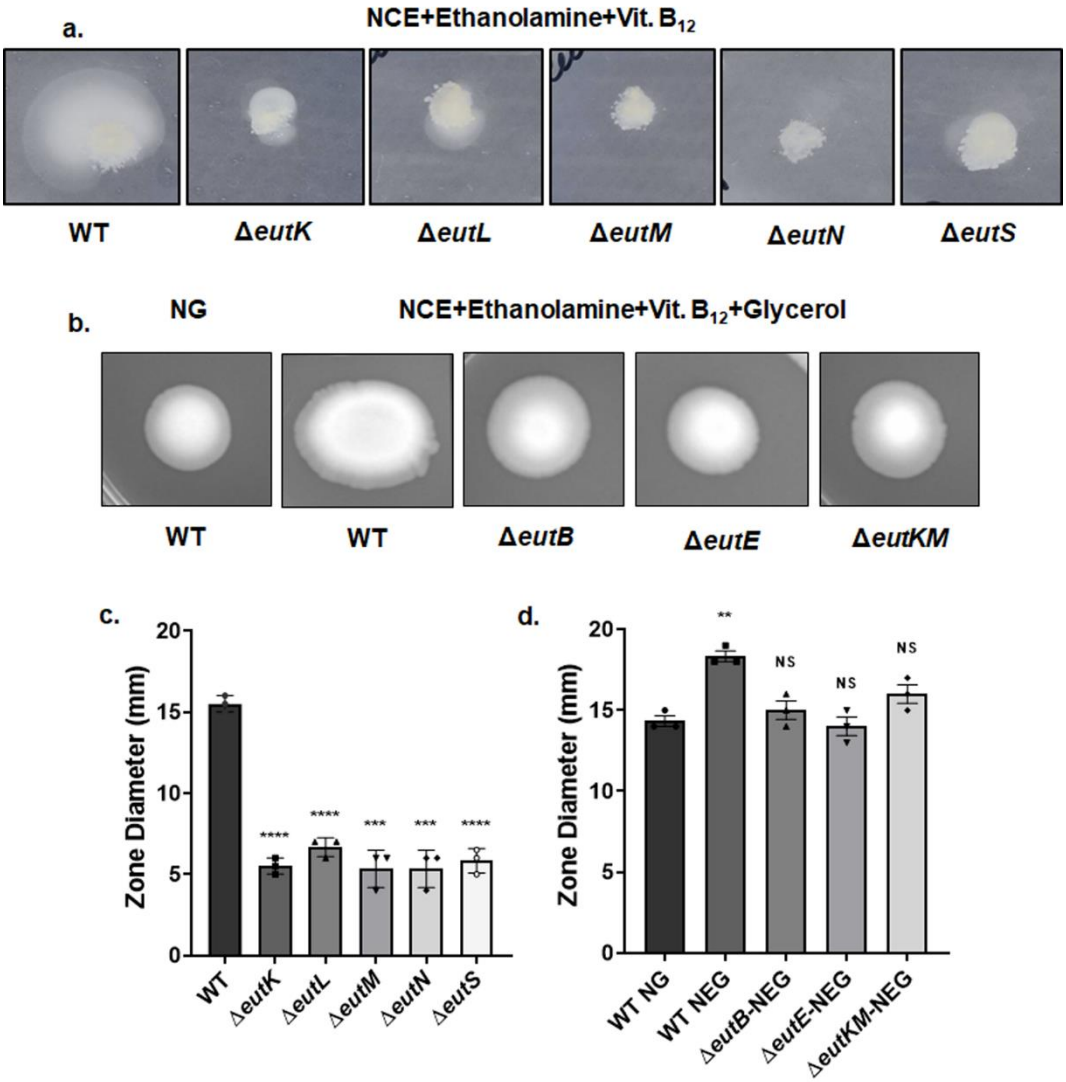


**Fig. 5.** Swarming Motility a) Diameter of colonies of shell protein mutants measured against WT. b) Addition of Ethanolamine in glycerol-containing media enhances the motility of WT. c) The zone diameter of WT was measured compared to shell protein mutants grown in minimal media containing ethanolamine as a carbon source. d) Measure the zone diameter of WT compared in media with and without ethanolamine supplemented with glycerol. An unpaired *t*-test (two-tailed) was used for statistical significance. NS $P > 0.05$, * $P < 0.05$, ** $P < 0.01$, *** $P < 0.001$, **** $P < 0.000$.

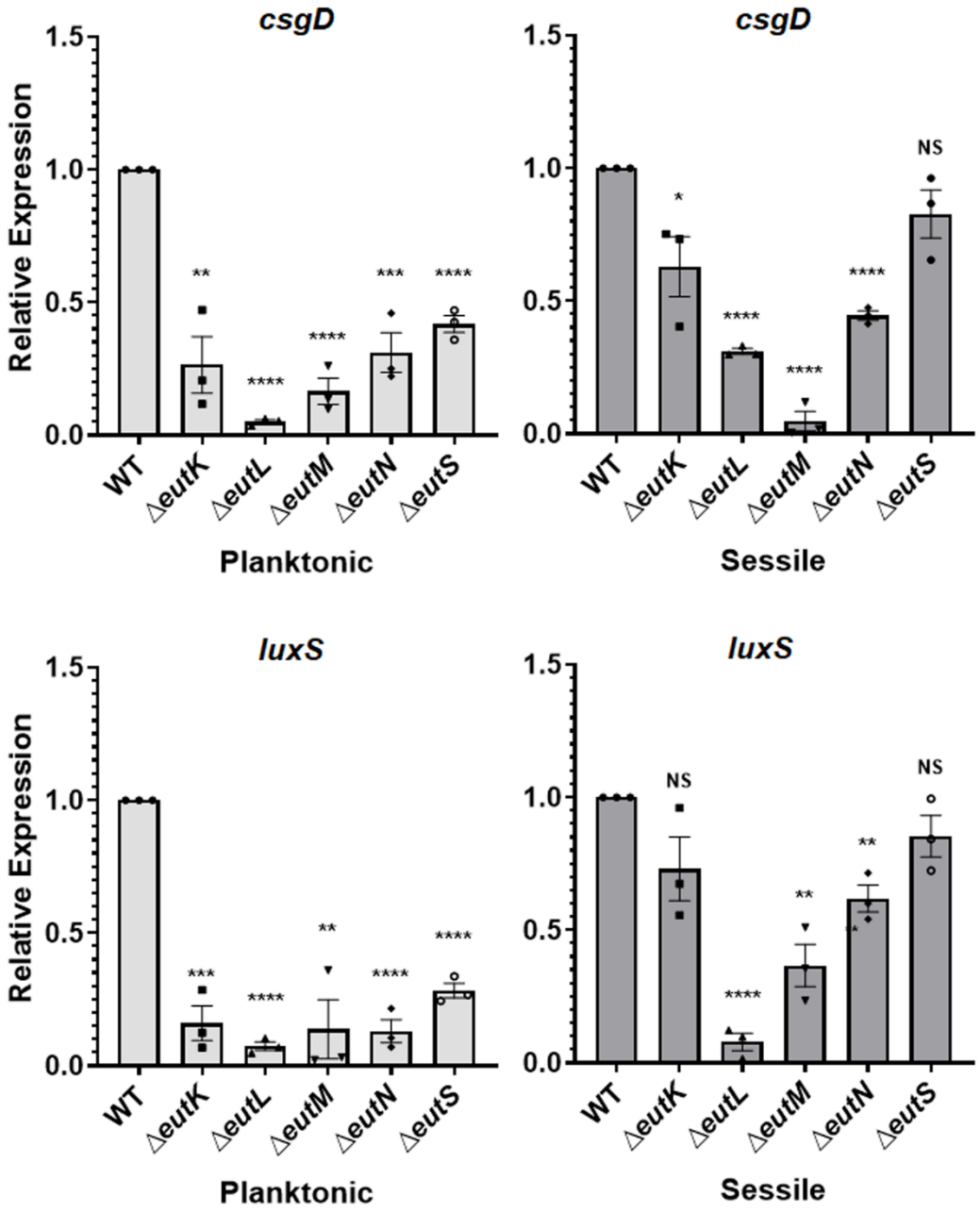
csgD
csgD
luxS
luxS
Relative Expression
1.5
1.0
0.5
0.0
WT
ΔeutK
ΔeutL
ΔeutM
ΔeutN
ΔeutS
Planktonic
Sessile
NS
*
**
***
****

909

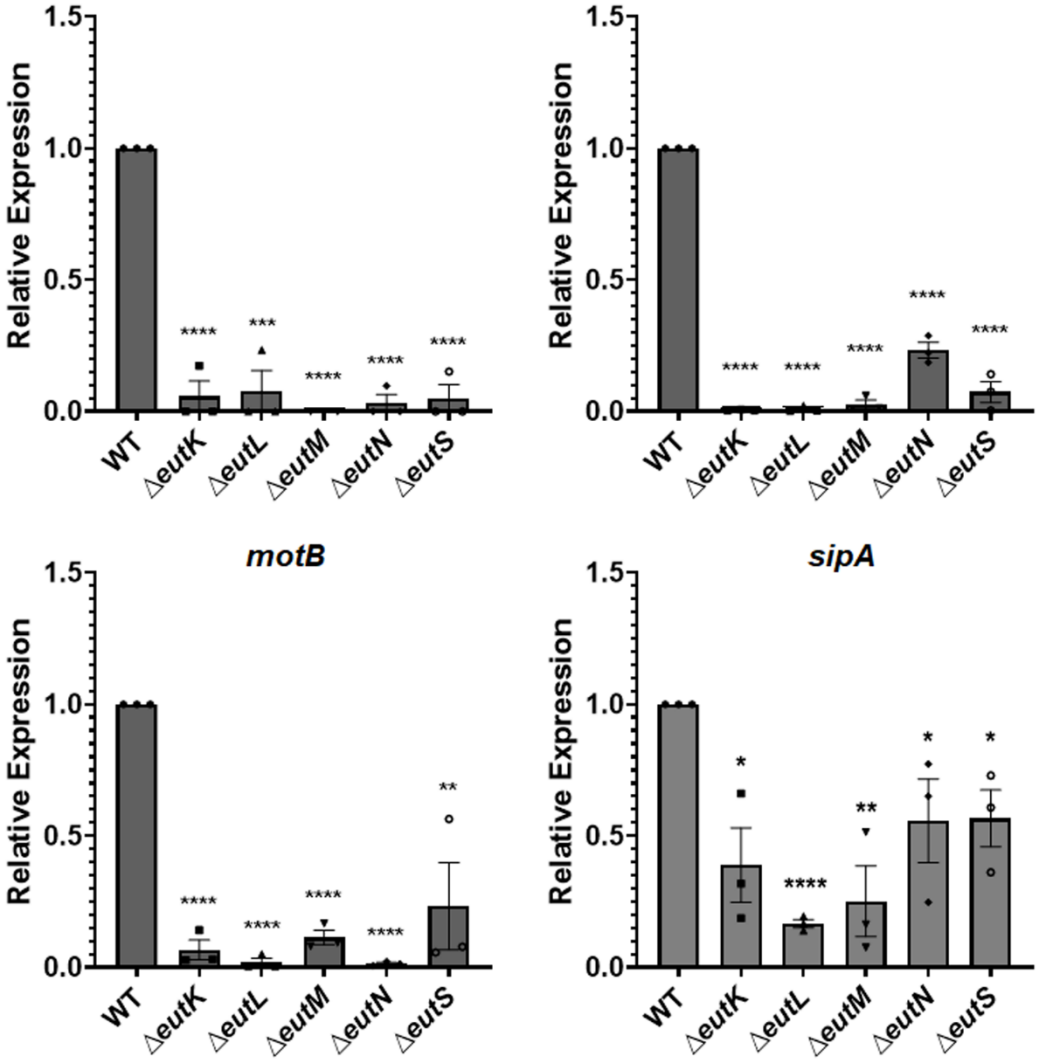


**Fig. 6.** Gene Expression Analysis of gene targets related to Biofilm, Motility, and Cell Invasion. An experiment was performed with three technical replicates and three biological replicates. An unpaired *t*-test (two-tailed) was used for statistical significance. NS P > 0.05, * P < 0.05, ** P < 0.01, *** P < 0.001, **** P < 0.000.

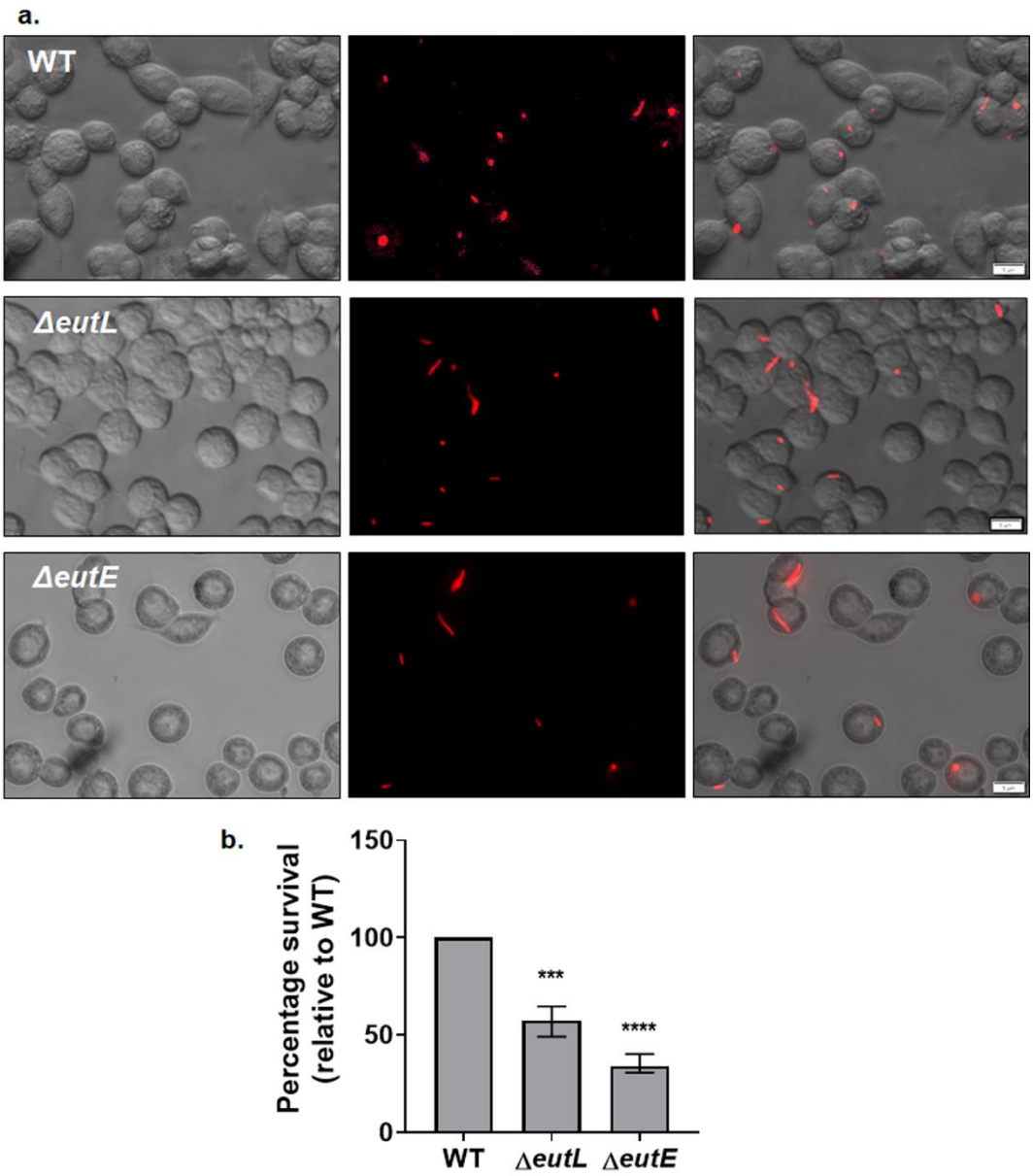


Fig 7. a) Visualization of intracellular bacteria in macrophage cells RAW264.7: Infection of the RAW264.7 cells with wild-type, *eutL*, and *eutE* mutant strains of *Salmonella* (50 MOI) expressing m-Cherry (red). A representative microscopy merged image shows a bright field with bacteria expressing m-Cherry. The imaging was done at four hours post-infection. b) Percentage of recovered bacterial cells after four hours of infection. The experiments were done in triplicate with three biological replicates. An unpaired *t*-test (two-tailed) was used for statistical significance. * $P < 0.05$, ** $P < 0.01$, *** $P < 0.001$, **** $P < 0.000$.